International Journal of Engineering Research in Africa
ISSN: 1663-4144, Vol. 53, pp 76-100
© 2021 Trans Tech Publications Ltd, Switzerland
Submitted: 2020-03-05
Revised: 2020-09-21
Accepted: 2020-10-15
Online: 2021-03-04

Numerical Verification of Strut and Tie Models and Failure Modes of Reinforced Self-Compacting Concrete Deep Beams

Mutiu Adelodun Akinpelu[1,a*], Bilyamin Adeoye Ibitoye[2,b], Samson Olalekan Odeyemi[3,c] and Kabir Opeyemi Olorede[4,d]

[1,2,3]Department of Civil and Environmental Engineering, College of Engineering and Technology, Kwara State University, Malete, Kwara State, Nigeria.

[4]Department of Statistics and Mathematical Sciences, College of Pure and Applied Sciences, Kwara State University, Malete, Kwara State, Nigeria.

[a*]mutiu.akinpelu@kwasu.edu.ng, [b]bilyamin.ibitoye@kwasu.edu.ng, [c]samson.odeyemi@kwasu.edu.ng, [d]Kabir.olorede@kwasu.edu.ng

Keywords: Deep Beams, Strut and Tie Model, Failure Modes, Damage Plasticity.

Abstract. This study utilized Finite Element Method (FEM) to analyse the structural behaviour and failure modes of Reinforced Self Compacting Concrete (RSCC) deep beams. Eighteen deep beam specimens subjected to four-point loadings were modelled and analyzed using Abaqus modelling tool. Damage plasticity model was used to characterised the nonlinear behaviour of concrete material while linear elastic, linear-plastic-hardening model represented the reinforcing steel material behaviour. The results of the finite model were compared with four different Strut and Tie Models (STMs) using one-way Analysis of Variance (ANOVA). Results of the numerical study revealed that the concrete strength and shear span to depth ratio mostly affect the load-deflection response of the beams. Also, the failure modes of the studied deep beams were influenced by shear span to depth ratio, concrete strength as well as web reinforcement distribution. The ANOVA results also showed that the FEM outperformed the existing STMs.

Introduction

Beams with small span to effective depth ratio are called deep beams. Although the definition of the limiting value of this ratio varies for different international design codes, the parameter has been widely adopted for classifying beams as either deep or slender. According to American Concrete Institute (ACI 318M) [2], a beam supporting uniformly distributed load is said to be deep when the ratio of its clear span to effective depth is less than or equal to four, while region of a beam between point load and face of the support is considered deep when the ratio of the shear span to effective depth is less than or equal to two. Eurocode 2 [3], on the other hand, categorized a beam as deep when the ratio of span to effective depth is less than or equal to three. Owing to the limited span to effective depth ratio, the strength of a deep beam is governed by shear rather than bending. This makes it desirable in heavily loaded structures including capping beams and foundations in bridges, water tanks, diaphragms, as well beams used in high-rise buildings to provide column offsets [4]. The web of a typical deep beam is narrow and contains overcrowded arrangement of reinforcements. Hence, it is difficult to achieve adequate compaction of concrete by the mechanical method as the material is placed through the web of the beam. This could result in structural defects in concrete structures namely: Segregation, honey-comb, void, weak bond with reinforcement bars as well as poor surface finish. These deficiencies can severely deteriorate the materials mechanical properties and thus, jeopardizing structural integrity and durability of the entire structure. In order to overcome the difficulties in achieving adequate and effective compaction of the conventional Vibrated Concrete (VC) by mechanical means, Self-Compacting Concrete (SCC) have been suggested for constructing narrow structural components such as deep beams [1]. However, evaluation of the structural performance of structures constructed with the newly introduced SCC is necessary considering the reported differences in its mechanical properties when compared to the VC. Research findings have shown that the aggregate interlock mechanism which represents a significant portion of the total shear

All rights reserved. No part of contents of this paper may be reproduced or transmitted in any form or by any means without the written permission of Trans Tech Publications Ltd, www.scientific.net. (#552664491-18/02/21,06:55:57)

strength of concrete is suggested to be less effective in SCC due to lower volume and smaller sizes of the coarse aggregate in the SCC [5]. Furthermore, the modulus of elasticity of SCC, which is required for accurate estimation of deflections, shrinkage, creep, as well as prestress losses, has also been found to be less than that of vibrated concrete [6].

Apart from this, exact analysis of the complex stress distribution in the deep region of the beam cannot be evaluated using the basic assumption of the bending theory since the beam section is disturbed leading to nonlinear strain distribution across its depth [7]. Strut and Tie Model (STM) is the most recent approach for the analysis and design of D-regions. It is an approximate method in which the continuous regions of reinforced concrete are converted to corresponding truss configurations. The compression and tension zones are transformed to equivalent struts and ties respectively which are joined at the nodal points to create a truss configuration that can be effectively analysed with the equations of statics [2]. It is however worthy to state that the current STM for designing deep beams has been formulated based on the parameters of VC. Also, STM has not been widely implemented due to some identified limitations. There is difficulty in fixing an optimum truss configuration for a given structural member with given loading due to lack of adequate understanding of the load transfer mechanism in the disturbed region [8], [9]. Couple with this, STM only offers approximate solutions by simplifying the complex stress state in D-region in a simple truss leading to conservative results and also, it cannot predict the failure modes of deep beams. Therefore, there is need to improve on the existing design procedure for reinforced concrete deep beam especially when SCC is involved.

Experimental testing of scaled specimens has been the trend in evaluating the parameters influencing the structural response of members since it provides real life behaviour of structures. Nevertheless, the need to perform the laboratory tests according to set standards makes the procedure cumbersome, time wasting and costly. Application of numerical procedure in the modeling and simulation of structural response of members is a trending issue in structural Engineering research. Among all, Finite Element Method (FEM) is the most widely adopted numerical technique for structural analysis. The availability of numerous material models which can be easily coupled with FEM has also make the method very desirable. Hence, the present work studied the failure modes of RSCC deep beams using FEM.

Strut and Tie Models

Many STMs are reported in literature for the design of deep beams. The governing equations and the major assumptions of the STMs compared in this study are presented in the section. The STMs considered include ACI 318M model [2], Eurocode 2 model [3], Al-Khafaji et al. model [1] and Arabzadeh et al. model [10].

ACI 318M STM. ACI 318M [2] recommends using the strut and tie methods for designing deep beams which require the use of depth of strut and strength of node as presented in Fig. 1.

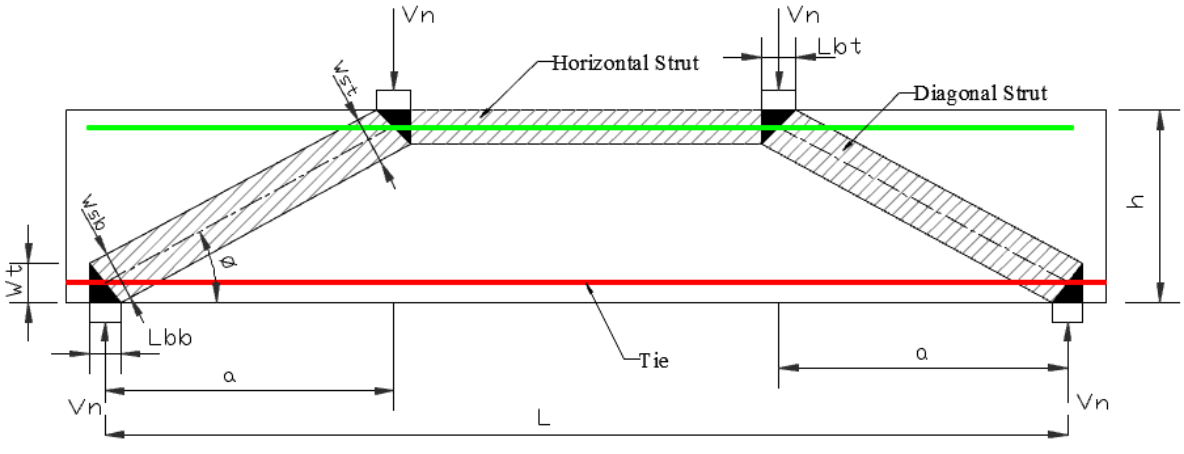


Fig. 1: STM analogy of a deep beam

The nominal strut strength in compression, F_{ns}, is expressed as the smaller value of (a) or (b) at the two ends of the strut.

(a) Strut without longitudinal reinforcement

$$F_{ns} = f_{ce}A_{cs} \quad (1)$$

(b) Strut with longitudinal reinforcement

$$F_{ns} = f_{ce}A_{cs} + f_y'A_s' \quad (2)$$

$$A_{cs} = bw_s \quad (3)$$

where: f_y' and A_s' are yield strength and area of compression reinforcement respectively, A_{cs} is the cross-sectional area at one end of the strut and b is the width of the beam.

w_s is the width of the strut which is equal to w_c for horizontal strut or the smaller of w_{sb} or w_{st} for the diagonal strut as shown in Fig. 1.

$$w_{sb} = w_t \cos\theta + l_{bb} \sin\theta \quad (4)$$

$$w_{st} = w_c \cos\theta + l_{bt} \sin\theta \quad (5)$$

f_{ce} is the lesser of the effective compressive strength of concrete in the strut and nodal zone as expressed in equations 6 and 8 respectively.

The effective strength of a strut is given as:

$$f_{ce} = 0.85\beta_s f_c \quad (6)$$

The parameter β_s accounts for the reduction effect of cracked concrete and web reinforcement on strut strength.

The nominal compression strength of a nodal zone, F_{nn}, is given as

$$F_{nn} = f_{ce}A_{nz} \quad (7)$$

Where f_{ce} is the effective compressive strength of the concrete in the nodal zone given as:

$$f_{ce} = 0.85\beta_n f_c \quad (8)$$

A_{nz} is the smaller of (a) and (b):

(a) The area of the face of the nodal zone on which F_u acts, taken perpendicular to the line of action of F_u;

(b) The area of a section through the nodal zone, taken perpendicular to the line of action of the resultant force on the section.

The nominal strength of a tie, F_{nt}, can also be obtained from

$$F_{nt} = A_{ts}f_y \quad (9)$$

Where A_{ts} and f_y are the area and yield strength of tensile reinforcement respectively.

Eurocode 2 STM. Unlike the ACI 318M equation which accounts for the effect of strut shapes, Eurocode 2 [3] accounts for the effect of transverse strain on strut capacity by introducing strength reduction factor, v. The design strength of a strut with transverse tensile strain is expressed as

$$\sigma_{RDmax} = 0.6vf_{cd} \tag{10}$$

where: ν is a strength reduction factor for concrete cracked in shear given as

$$v = 1 - {}^{f_c}/_{250} \tag{11}$$

f_{cd} is the designed compressive strength of concrete expressed as

$$f_{cd} = \propto_{cc} f_c/\gamma_c \tag{12}$$

$\propto_{cc}$ is the coefficient taking account of creep effects on the compressive strength of concrete. The recommended value is 1.0, γ_c is the partial factor safety for concrete stated as 1.5
The designed nodal strength considers the node types and it is expressed as follows:

$$\sigma_{RDmax} = kvf_{cd} \tag{13}$$

where: σ_{RDmax} is the maximum stress applicable to the surfaces of the node.

Arabzadeh et al. STM. Arabzadeh et al.[10] presented a modified STM to evaluate shear strength of deep beams. The model governing equation is based on the assumption that the shear strength of deep beams depends on two independent variables including the diagonal concrete strut due to the strut and tie mechanisms, and the corresponding resisting force perpendicular to the strut due to web reinforcements.
The model equation for the nominal compressive strength in the strut, F_{ns}, is similar to ACI 318M model and its given as:

$$F_{ns} = f_{ce}A_{cs} \tag{14}$$

where:

$$f_{ce} = \mathrm{v}_{cw}f_c \tag{15}$$

$$v_{cw} = v_c + v_w \tag{16}$$

where v_c is the strength efficiency factor in the absence of web reinforcement and v_w accounted for the reduction effect of the factor on the strut strength due to web reinforcements.
The nonlinear model for calculating strength efficiency factor, v_{cw} is given as:

$$v_{cw} = \frac{f_c^{-0.3}}{0.5+0.1(\frac{a}{d})^2} + 0.09{\rho_p}^{0.65}\left(\frac{f_{yw}}{f_c}\right)\left(\frac{a}{w_s}\right)\frac{1}{\sin\theta} \tag{17}$$

where:

$$\rho_p = \rho_v A_v \cos^2\theta + \rho_h A_h \sin^2\theta \tag{18}$$

$\rho_v = A_v/bn_v s_v$, $\rho_h = A_h/bn_h s_h$, A_v and A_h are the areas of the vertical and horizontal web reinforcements, s_v and s_h are vertical and horizontal web reinforcement spacing, n_v and n_h are the number of vertical and horizontal reinforcements respectively. Other parameters are as previously defined.

Al-Khafaji et al. STM. Al-khafaji et al. [1] also derived STM for estimating the ultimate load of RSCC deep beams. The adopted truss model is the same as ACI 318M model shown Fig. 1. The author argued that the ACI 318M equation does not account for the influence of web reinforcement on the shear strength. Therefore, the predicted shear capacity represents only the concrete shear strength (V_c) but not the total shear strength (V_n) as shown in the Fig. 1. In the absence of web reinforcements, the failure criteria based on the combination of tension (tie) and compression strut failure criterion is stated as

$$\frac{V_c}{V_{cc}} + \frac{V_c}{V_{ct}} = 1 \tag{19}$$

where Vc is the applied shear force

$$V_{cc} = F_{ns} \sin\theta \tag{20}$$

$$V_{ct} = F_{nt} \tan\theta \tag{21}$$

F_{ns} and F_{nt} are as previously defined.

$$\theta = \tan^{-1}\frac{d-d'}{a} \tag{22}$$

The nonlinear form of equation 19 is adopted by raising terms of the equation to a constant denoted by C1 as expressed in equation (23)

$$\left(\frac{V_c}{V_{cc}}\right)^{c_1} + \left(\frac{V_c}{V_{ct}}\right)^{c_1} = 1 \tag{23}$$

Therefore,

$$V_c = {V_{cc}V_{ct}}\Big/{\sqrt[c_1]{(V_{cc})^{c1} + (V_{ct})^{c1}}} \tag{24}$$

The contribution of the web reinforcement to the shear strength is given as:

$$V_s = \left(C_2\frac{a}{d}\rho_v f_{yv} + \left(C_3 - \frac{a}{d}\right)\rho_h f_{yh}\right) bd \tag{25}$$

where f_{yv} and f_{yh} are the yield of strength of vertical and horizontal web reinforcements.
Hence, the total shear strength (V_n) is:

$$V_n = V_c + V_s \tag{26}$$

The coefficients C_1, C_2 and C_3 are given as 2, 1 and 3 respectively.

Methodology

Study Approach. In order to achieve the set objectives, the study was implemented in two parts. The first part involved numerical modelling of reinforced concrete deep beam using Abaqus finite element modelling tool and comparison of the model outputs with laboratory observations. Two deep beams previously experimented by Choi et al. [11] were selected as a reference. In the second part, numerical simulation was conducted to evaluate various parameters affecting the shear behaviour of reinforced concrete deep beams.

Finite Element Study. The general purpose FE software, Abaqus [12] was used to develop the FE model used to mimic the structural behavior of RSCC deep beams. The material constitutive models and all the modeling assumptions as implemented in this study are briefly discussed in the subsequent sections.

Material Constitutive Models. For the presented study, Concrete Damage Plasticity Model (CDPM) as incorporated in Abaqus software was utilized to simulate plastic damage of concrete. The model has been successfully applied in the analysis of various reinforced concrete structures and was reported to be very effective in capturing reinforced concrete behaviour up till failure. [13], [14] . The earlier formulation of CDPM was conceived by Lubliner et al. [15] and later improved by Lee and Fenves [16]. CDPM is premised on the assumption that the main two failure mechanisms are tensile cracking and crushing of concrete in compression.

The model governing equations for the uniaxial tensile and compressive stress-strain behaviour of concrete are as presented in equations 29 and 30.

$$\sigma_t = (1 - d_t)E_0\left(\varepsilon_t - \tilde{\varepsilon}_t^{pl}\right) \tag{27}$$

$$\sigma_c = (1 - d_c)E_0\left(\varepsilon_c - \tilde{\varepsilon}_c^{pl}\right) \tag{28}$$

where E_0 is the initial (undamaged elastic stiffness) and $\tilde{\varepsilon}_c^{pl}$, $\tilde{\varepsilon}_t^{pl}$, $\tilde{\varepsilon}_c^{in}$, $\tilde{\varepsilon}_t^{in}$ are the compressive plastic strain, tensile plastic strain, compressive and tensile inelastic strain respectively.
Application of CDPM in Abaqus requires large data inputs although most of the data can be readily obtained using mathematical models. Detailed description of the input parameters and the required mathematical models have been presented elsewhere [17]. Table 1 gives the details of the materials constitutive model parameters adopted in the study.

Table 1: Material constitutive model parameters

Material	Parameter
Concrete	Model – CDPM Poisson ratio = 0.2 Dilation Angle, ψ = 56˚ (Akinpelu & Adedeji, 2018) Viscosity, μ = 0.0001 (Michał & Andrzej 2015) Flow Potential Eccentricity = 0.1 (Jankowiak & Odygowski, 2005) Stress ratio = 1.16 (Default Value) K = 0.667 (Default Value) Compressive stress-stress data = Eurocode 2, 2004 model Tensile stress – strain data = Cornelissen et al., 1986 (as cite in Genikomsou & Polak, 2016)
Rebar	Model – Linear elastic, linear strain hardening model Young modulus, Es = 210 N/mm^2 Poisson ratio = 0.3

Element Types and Meshing. For this simulation study, the concrete and the steel loading plate were modelled with three dimensional 8-node linear solid element with reduced integration (C3D8R) while the rebars are modelled with three dimensional 2-node linear truss element (T3D2) since they resist only axial stresses (Fig. 2). The plate was introduced in the support region to prevent local stress concentrations. Abaqus does not recognize mechanical contact or proximity between part instances or regions of an assembly unless that contact has previously been defined in the interaction module. Hence, the bonding of reinforcement with the concrete element was modelled with an embedded constraint available in the Abaqus interaction module while the loading plates and the beam element were also connected with tie constraint. The loadings were applied using a displacement control.

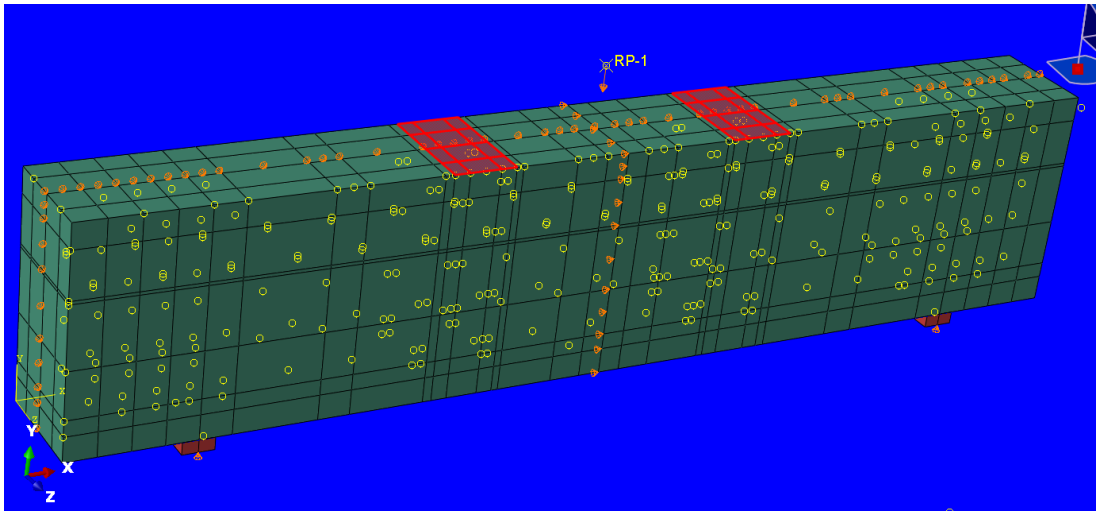


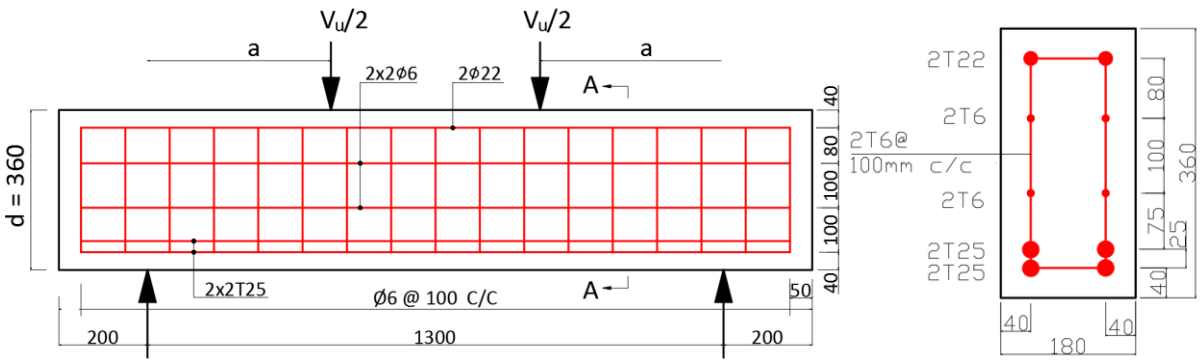
Fig. 2: Typical FE model of deep beam specimen showing the boundary conditions and the loading surface

Parametric Study

Eighteen deep beams were modeled and analyzed under 4-point loadings. The parameters investigated were the concrete compressive strength (f_c), shear span to effective depth ratio (a/d), vertical and horizontal web reinforcement ratio (R_v and R_h). Detail of the beam dimensions is shown in Fig. 3 while the properties of the specimens are detailed in Table 2.

Table 2: Detailed configuration of the modelled deep beam specimens

Beam Code	Length (mm)	Cross section (mm)	f_c (N/mm^2)	a/d	Reinforcements			
					Tension	Compression	Vertical web	Horizontal web
B1	1700	180 x 360	52.10	0.7	2x2ϕ25	2ϕ20	ϕ6/100	ϕ6/100
B2	1700	180 x 360	52.10	1.4	2x2ϕ25	2ϕ20	ϕ6/100	ϕ6/100
B3	1700	180 x 360	52.10	2.0	2x2ϕ25	2ϕ20	ϕ6/100	ϕ6/100
B4	1700	180 x 360	52.10	0.7	2x2ϕ25	2ϕ20	ϕ6/100	ϕ6/50
B5	1700	180 x 360	52.10	1.4	2x2ϕ25	2ϕ20	ϕ6/100	ϕ6/50
B6	1700	180 x 360	52.10	2.0	2x2ϕ25	2ϕ20	ϕ6/100	ϕ6/50
B7	1700	180 x 360	52.10	0.7	2x2ϕ25	2ϕ20	ϕ6/50	ϕ6/100
B8	1700	180 x 360	52.10	1.4	2x2ϕ25	2ϕ20	ϕ6/50	ϕ6/100
B9	1700	180 x 360	52.10	2.0	2x2ϕ25	2ϕ20	ϕ6/50	ϕ6/100
B10	1700	180 x 360	52.10	0.7	2x2ϕ25	2ϕ20	ϕ6/50	ϕ6/50
B11	1700	180 x 360	52.10	1.4	2x2ϕ25	2ϕ20	ϕ6/50	ϕ6/50
B12	1700	180 x 360	52.10	2.0	2x2ϕ25	2ϕ20	ϕ6/50	ϕ6/50
B13	1700	180 x 360	26.05	0.7	2x2ϕ25	2ϕ20	ϕ6/50	ϕ6/50
B14	1700	180 x 360	26.05	1.4	2x2ϕ25	2ϕ20	ϕ6/50	ϕ6/50
B15	1700	180 x 360	26.05	2.0	2x2ϕ25	2ϕ20	ϕ6/50	ϕ6/50
B16	1700	180 x 360	26.05	0.7	2x2ϕ25	2ϕ20	ϕ6/100	ϕ6/50
B17	1700	180 x 360	26.05	1.4	2x2ϕ25	2ϕ20	ϕ6/100	ϕ6/50
B18	1700	180 x 360	26.05	2.0	2x2ϕ25	2ϕ20	ϕ6/100	ϕ6/50



(a) Beam longitudinal section (b) Section A-A

Fig. 3. Typical experimental setup for the modelled deep beam specimen (Specimen B1*)*

Comparative study. The experimental data structure and research interest in determining whether or not there is statistically detectable differences among the shear strength of deep beams obtained from Finite Element Method (FEM) and the four Strut and Tie Models (STMs) including ACI 318M [2], Eurocode 2 [3], Arabzadeh et al. [10] and Al-khafaji et al. [1] informed the choice of adopting the statistical method called One-way Analysis of Variance (ANOVA) [21], described in equation (31).

$$y_{ij} = \mu + \alpha_i + \epsilon_{ij} \tag{29}$$

where,
y_{ij} = Observation arising from ith sample beam as measured by method j
μ = Overall or grand average shear strength measurement
α_i = Effect of model j
ϵ_{ij} = ijth random error term
The ANOVA (equation 31) remains valid as long as samples observations are independent and identically distributed with mean 0 and constant variance σ^2 i.e. $\epsilon_{ij} \sim N(0, \sigma^2)$ and assuming fixed effects for parameters.

Null Hypothesis($\boldsymbol{H_0}$): There is no statistically detectable difference among the five models in terms of their ultimate beam strength estimates

Alternative Hypothesis($\boldsymbol{H_a}$): Not H_0.

For one-way ANOVA specified for this study, samples are assumed to come from normal distribution. The variances are not necessarily assumed to be equal. To inspect the data sample for normality, multivariate test of normality was conducted at 5% critical rejection region, using Royston statistics [22] from the R software function *MVN* in the *MVN* libraries [23]. Nonparametric equivalent of the parametric one-way ANOVA called Kruskal Wallis Rank Sum Test [24] was adopted where violations of normality assumption was observed.
Wherever the test was confirmed significant with 95% confidence, Tukey Honest Significant Differences Test (TukeyHSD) [25], [26] were adopted to further investigate which particular pair(s) of models exhibit significantly different prediction of shear strength of deep beam. All computations and analyses were done, using version 3.5.0. [27] of the R software for statistical computing and graphics.

Results and Discussion

Model Calibration and Validation. As stated earlier stated, the finite element model adopted in the present study has been validated by comparing the model outputs with laboratory results of two deep beams previously studied by [11]. The model was evaluated in term of cracking and failure

loads, failure pattern and load-deflection response. The results of the model calibration and validation have been published elsewhere [17].

Parametric Study. The simulation results for the 18 deep beams modelled in the numerical study are summarised in Table 3. The parameters R_v and R_h are vertical web reinforcement ratio horizontal web reinforcement ratio respectively.

Table 3: Summary of Parametric study results

Beam Code	f_c (N/mm^2)	R_v %	R_h %	a/d	V_c (kN)	V_u (kN)	V_c/V_u
B1	52.10	0.31	0.31	0.7	379	1524.0	0.25
B2	52.10	0.31	0.31	1.4	349	712.0	0.49
B3	52.10	0.31	0.31	2.0	349	630.0	0.55
B4	52.10	0.31	0.63	0.7	364	1417.0	0.26
B5	52.10	0.31	0.63	1.4	344	741.0	0.46
B6	52.10	0.31	0.63	2.0	338	665.0	0.51
B7	52.10	0.63	0.31	0.7	368	1315.0	0.28
B8	52.10	0.63	0.31	1.4	338	826.0	0.41
B9	52.10	0.63	0.31	2.0	344	689.0	0.50
B10	52.10	0.63	0.63	0.7	366	1289.0	0.28
B11	52.10	0.63	0.63	1.4	349	884.0	0.39
B12	52.10	0.63	0.63	2.0	346	715.0	0.48
B13	26.05	0.63	0.63	0.7	235	741.0	0.32
B14	26.05	0.63	0.63	1.4	203	625.0	0.32
B15	26.05	0.63	0.63	2.0	201	606.0	0.33
B16	26.05	0.31	0.63	0.7	202	832.0	0.24
B17	26.05	0.31	0.63	1.4	194	528.0	0.37
B18	26.05	0.31	0.63	2.0	186	497.0	0.37

Effect of shear-span to effective depth ratio (a/d). The influence of a/d on the Vc and Vu is discussed in this section. The Vc for the tested beam series as listed in table 4.3 were obtained in the visualisation module of the numerical model by monitoring the occurrence of the tensile and the compressive damage in the FE model. The load corresponding to the appearance of the first diagonal tensile damage in the shear span was recorded as the diagonal cracking load. At this analysis stage for all the simulated deep beams, the propagation of compressive damage has not occurred. It is therefore adequate to conclude that the diagonal crack is a tensile failure. Fig. 4 shows the variation of normalised diagonal crack load with a/d ratio for different combination of web reinforcements. Where a/d is less than 1.5, the Fig. indicates that the normalised diagonal cracking load generally decreases with a/d ratio although the rate of the decrement is influenced by web reinforcement quantity. Where a/d ratio is greater than 1.5, the normalised cracking load increases with increasing a/d ratio for specimens with low horizontal web reinforcement value. For deep beams with high horizontal web reinforcement ratio, the diagonal cracking load generally decreases with the increasing a/d ratio. The result of the experimental work of Al-Khafaji et al. [1] on the shear behaviour of RSCC deep beams with a/d ratio of 0.6 and 1 also indicated that the diagonal cracking load slightly decreases with increasing a/d ratio.

The curves in Fig. 5 show the variation of ultimate shear strength with respect to shear span to effective depth ratio. Since each of the curves represents different amount of web reinforcements, the distributions of the reinforcements in the beams cover the practical range of vertical and horizontal web reinforcement ratio. From the Fig., the normalised shear strength of the beams generally decreases with increasing a/d ratio. The rate of decrement is larger for two cases with low vertical web reinforcement ratio (Rv = 0.0031). Other researchers have also reported similar trend [1], [28]. Therefore, it can be inferred that the influence of R_v becomes more significant for ultimate strength comapred to R_h as a/d ratio increases.

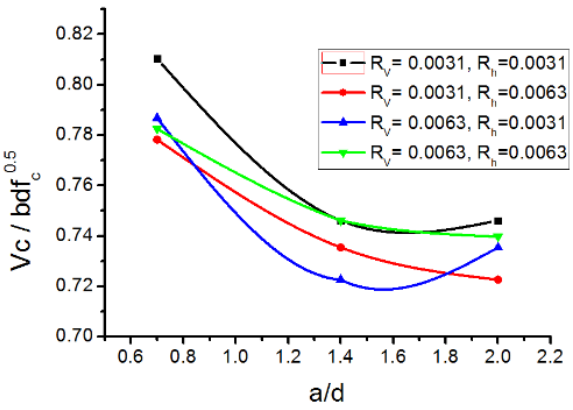


Fig. 4: Effect of a/d on V_c

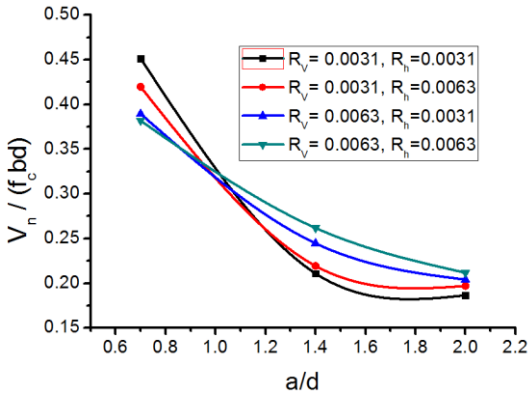


Fig. 5: Effect of a/d on V_n

Fig. 6 also shows the influence of shear span to effective depth ratio on the load deflection response of deep beams for different combination of web reinforcements. The load deflection response reduce with increasing shear span for all the loading regimes irrespective of the web reingorcement ratio. Fig. 6 further established the fact that the failure of a deep beam with low shear span (a/d = 0.7) is brittle in nature as the load deflection curve terminates abruptly. As the shear span increases the failure become more ductile as seen in the load deflection graph.

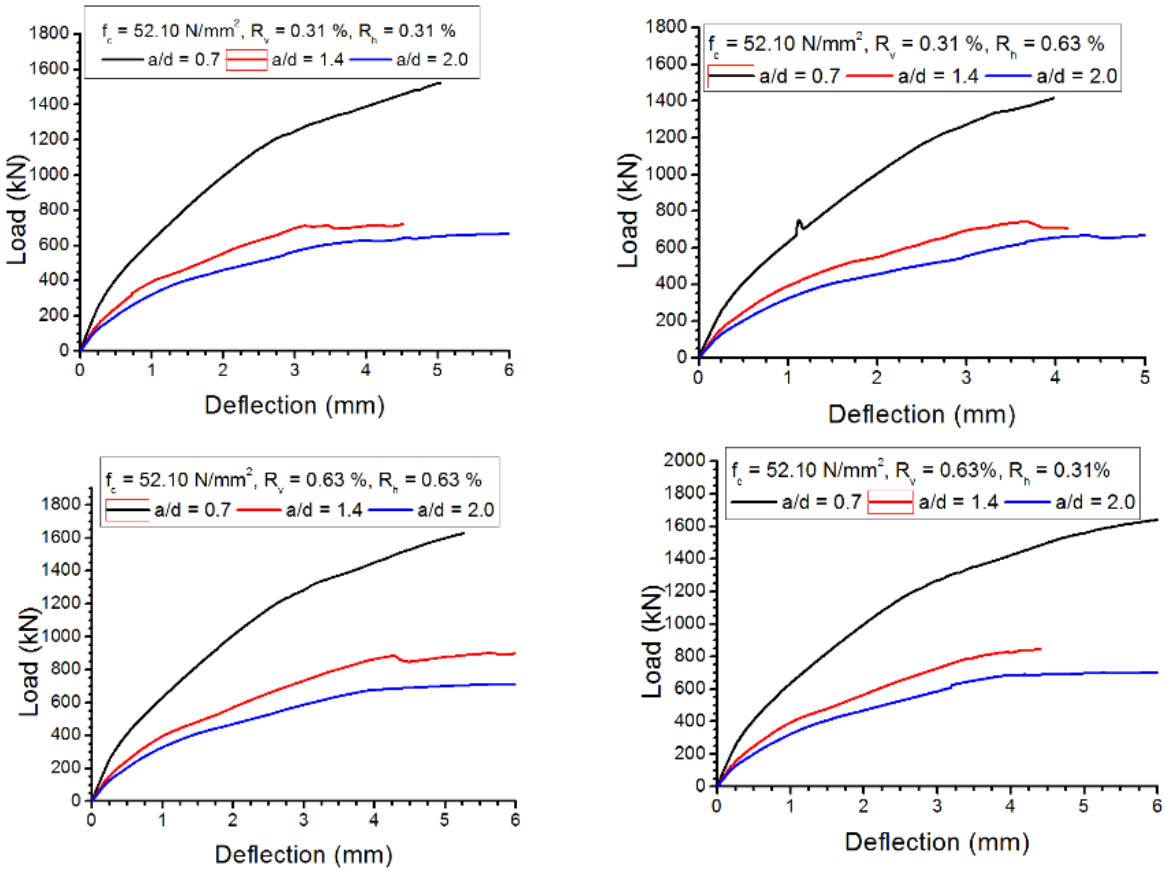


Fig. 6: Effect of shear span on the load deflection response

Parametric effect of f_c on the failure loads. The impact of the variation in concrete strength (f_c) on the diagonal cracking and failure loads of the studied beam specimens is shown in Table 4. The percentage increment in the failure load due to 100 % increment in f_c parameter varies from 42.51 % at low a/d ratio to 15.24 % at high a/d ratio. This means that the influence of f_c on deep beam strength reduces as a/d ratio approaches the limiting value of 2.0. The percentage increment is also influenced by vertical web reinforcement ratio (R_v). At a/d ratios of 0.7 and 1.4, the percentage

increment improves with increasing R_v ratio. However, where a/d is 2.0, increase in R_v ratio led to negative influence on the percentage increment of the ultimate load. The diagonal cracking load also increased from 35.79 % to 44.97 % due to doubling of f_c. Although the observed increment slightly reduced with increasing horizontal web reinforcement. Evaluation of the data presented in the Table 7 also revealed that the ratio of diagonal cracking to ultimate failure load (V_c/V_u) improved appreciably with increasing f_c.

Table 4: Effect of concrete strength on the failure loads

a/d	R_v %	f_c = 26.05 N/mm^2			f_c = 52.10 N/mm^2			% Change in failure load	
		V_c (kN)	V_u (kN)	V_c/V_u	V_c (kN)	V_u (kN)	V_c/V_u	V_c	V_u
0.7	0.0031	202	832	0.24	364	1417	0.26	44.51	41.28
	0.0063	235	741	0.32	366	1289	0.28	35.79	42.51
1.4	0.0031	194	528	0.37	344	741	0.46	43.60	28.74
	0.0063	203	625	0.32	349	884	0.39	41.83	29.30
2	0.0031	186	497	0.37	338	665	0.51	44.97	25.26
	0.0063	201	606	0.33	346	715	0.48	41.91	15.24

The influence of f_c on the load-deflection response is as shown in Fig. 7. It can be observed from the graphs in Fig. 7 that the reduction in concrete strength negatively affect the load-deflection response throughout the loading trend. This could be linked to the fact that the concrete strength contributes to the flexural rigidity of the beams by increasing the elastic modulus of the material. Similar result was observed by other researchers [1].

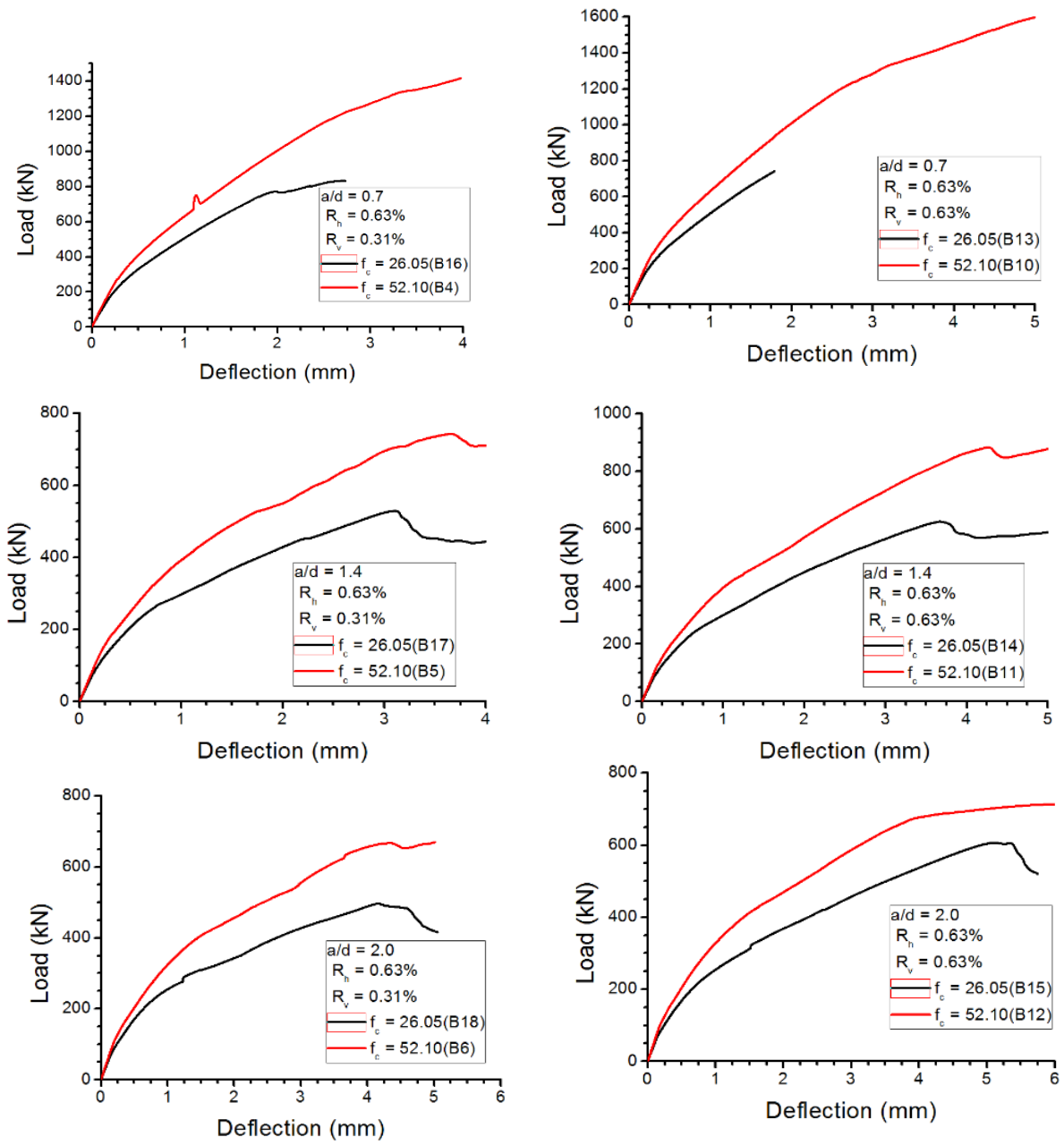


Fig. 7: Effect of f_c on load-deflection response

Parametric effect of R_v on the failure loads. The parametric influence of R_v on the appearance of diagonal tension crack and the ultimate failure of the beams is shown in Table 5. Where a/d ratio is very small (a/d = 0.7), increasing R_v generally has negative influence on the load carrying capacity of the analysed deep beams. The percentage decrease in the ultimate load due to doubling of R_v ranges from approximately 10 % to 16.0 %. The percentage reduction in strength slightly reduces with increasing horizontal web reinforcement ratio (R_h). The implication is that at low shear span (a/d = 0.7), high vertical web reinforcement ratio is not beneficial to the ultimate strength of deep beams. This behaviour could be linked to the effective transverse compressive stress that exists in concrete under low a/d ratio. Additional web reinforcement ratio leads to relatively low compressive strain which in turn leads to more softening of the concrete and therefore reduced ultimate strength of the beams. This conclusion also agrees with the analytical report of Kong (2002) on reinforced concrete deep beam.

Where a/d ratio is large (a/d = 1.4 and 2.0), the ultimate strength of the beams increases with increasing R_v ratio. The percentage increment ranges between 7.0 % to 16.0 % (average increase of 11.4 %) due to doubling of R_v ratio. At constant a/d ratio of 1.4, the percentage increments also

increase with R_h ratio. This implies that combination of high horizontal web reinforcement ratio (R_v) is effective for a/d ratio of 1.4.
The influence of the vertical web reinforcement on the diagonal cracking load of the beams is erratic. The percentage increments in the diagonal cracking loads ranges between -3.3 % to 2.3 % due to doubling of the R_v ratio. This value can be considered insignificant. Mohammadhassani, et al. [29] have previously concluded that the appearance of diagonal crack is only influenced by the concrete compressive strength which is independent of web reinforcement ratio.

Table 5: Effect of R_v on diagonal cracking and ultimate load

a/d	R_h	R_v = 0.31 %			R_v = 0.63 %			% Change in failure load	
		V_c	V_u	V_c/V_u	V_c	V_u	V_c/V_u	V_c	V_u
0.7	0.0031	379	1524	0.25	368	1315	0.28	-2.99	-15.89
	0.0063	364	1417	0.26	366	1289	0.28	0.55	-9.93
1.4	0.0031	349	712	0.49	338	826	0.41	-3.25	13.80
	0.0063	344	741	0.46	349	884	0.39	1.43	16.18
2	0.0031	349	630	0.55	344	689	0.50	-1.45	8.56
	0.0063	338	665	0.51	346	715	0.48	2.31	6.99

The plots in Fig. 8 illustrates the influence of horizontal web reinforcement on the load deflection response of deep beams. As seen in Fig 8., change in vertical web reinforcement (R_v) ratio does not influence the load-deflection response at the initial stage of the analysis. The reason is that flexural behaviour is dominant at that stage and the web reinforcement is not contributing to the flexural resistance. However, as the analysis progresses, diagonal tension cracks developed in the shear span which disrupt the flexural behaviour and shear response becomes more dominant. The influence of the difference in web reinforcements is only noticed after the diagonal crack has fully developed. Therefore, it could be concluded that vertical web reinforcement is only active after the diagonal shear cracks have fully developed.

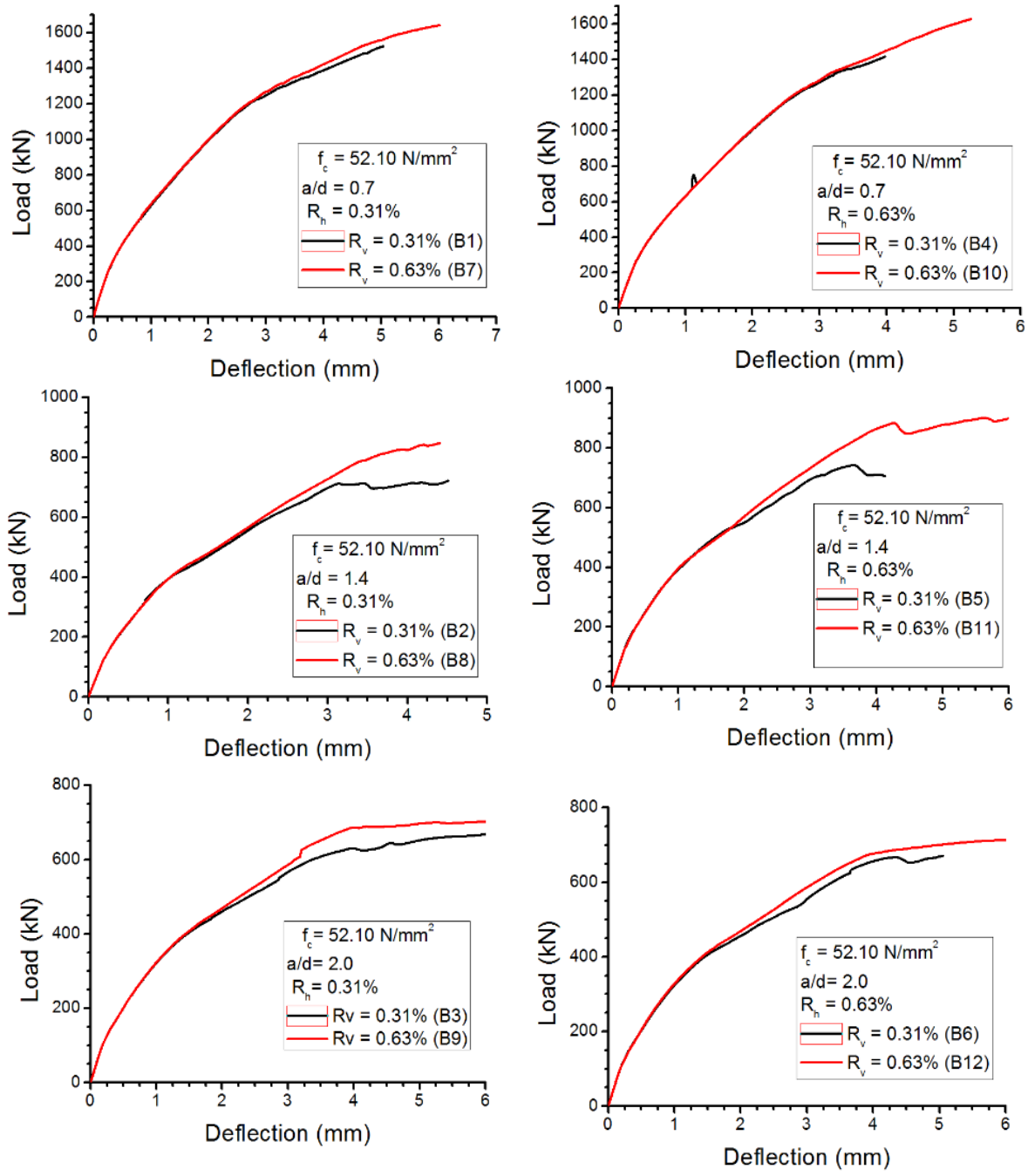


Fig. 8: Effect of R_v on load-deflection response

Parametric effect of R_h on failure loads. The parametric effects of R_h on the cracking and the ultimate loads of the beam specimens is computed in Table 6. Just like vertical web reinforcement (R_v), increase in R_h results in reduction of shear strength of beams having small a/d ratio (a/d = 0.7). Although the percentage reduction in strength due to change in R_h ratio is lower when compared to R_v ratio. The percentage decrease in ultimate load due to doubling of R_h ranges from 2.1 % to 7.6 % (average decrease of 4.9 %). The percentage decrement increases with increasing R_v ratio. ACI 318M, (2014) limits the minimum value of web reinforcement to 0.25 %. This result therefore established that increasing the web reinforcement ratio above the recommend minimum is not beneficial to deep beams having low a/d ratio of 0.7.

Where a/d ratio is greater than unity (a/d = 1.4 and 2) as seen in Table 9, increase in horizontal web reinforcement ratio slightly improves the ultimate strength of the beams. The percentage increase in strength ranges between 3.6 % to 6.6 % (average increase of 4.8 %). This result, however, indicates that the horizontal web reinforcement is less effective for member shear strength when compared to

vertical web reinforcement where doubling R_v lead to average of 11.4 % increase in shear strength. The ineffectiveness of horizontal web reinforcement in improving shear strength at high shear span is also reported in the experimental work of Al-Khafaji et al. [1] and Mohammadhassani et al. [30]. The influence of increasing R_h on the diagonal cracking load is erratic and unclear where it leads to percentage variation in strength ranging from -4.12 % to +3.15 %. Extensive experimental work is recommended to give adequate clarification on this.

Table 6: Effect of R_h on diagonal cracking and ultimate load

a/d	R_v %	R_h = 0.31 %			R_h = 0.63 %			% Change in failure load	
		Vc	Vu	Vc/Vu	Vc	Vu	Vc/Vu	Vc	Vu
0.7	0.0031	379	1524	0.25	364	1417	0.26	-4.12	-7.55
	0.0063	368	1315	0.28	366	1289	0.28	-0.55	-2.02
1.4	0.0031	349	712	0.49	344	741	0.46	-1.45	3.91
	0.0063	338	826	0.41	349	884	0.39	3.15	6.56
2	0.0031	349	630	0.55	338	665	0.51	-3.25	5.26
	0.0063	344	689	0.50	346	715	0.48	0.58	3.64

Fig. 9 shows the influence of horizontal web reinforcement ratios on the load deflection response of deep beams. It is obvious from the graphs (Fig. 9) that change in R_h has no impact on the load-deflection response of the evaluated beams. Hence, where R_h is similar, the load-deflection response converged. This is owing to the fact that the flexural rigidity of the beams does not depend on R_h and also, the effect R_h on the shear strength is very minimal as can be observed in Table 9.

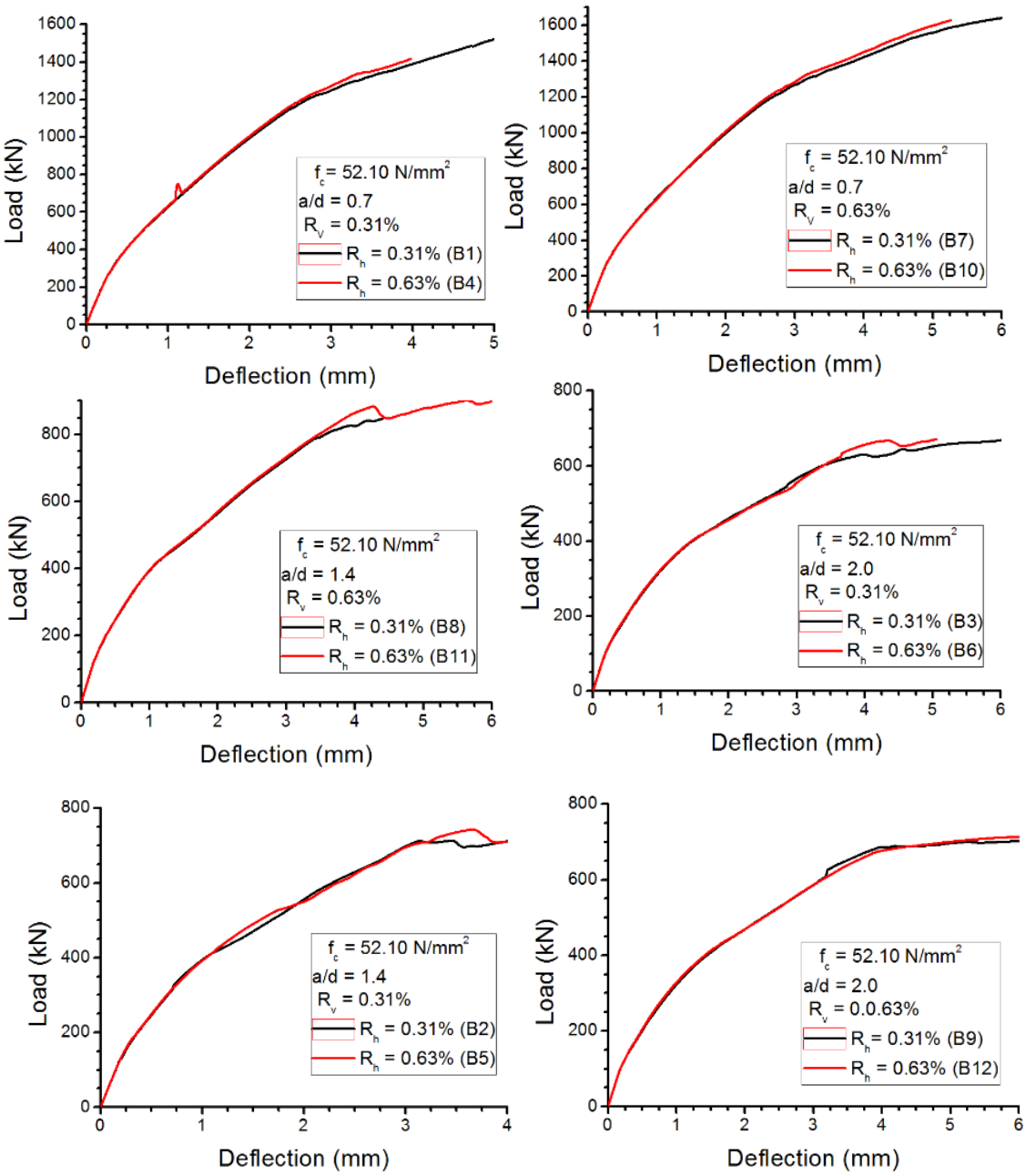


Fig. 9: Effect of R_h on load-deflection response

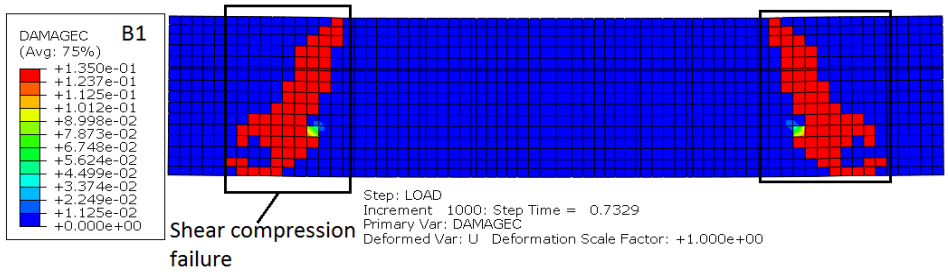
Failure Mechanisms in Deep Beam

The three types of shear failures numerically observed in the studied beam specimens are presented. These are: (i) Shear compression / Compression strut failure (ii) Diagonal splitting failure and (iii) Flexural tension failure.

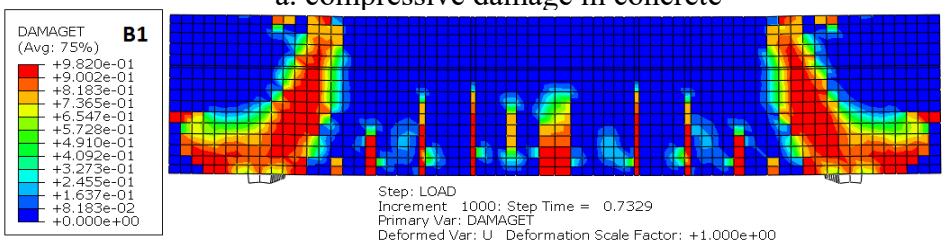
Shear Compression failure / Compression Strut failure. This mode of failure is found in deep beams with low shear span to effective depth ratio (a/d). It occurred in specimen B1, B4, B7, B10 and B16 (Fig. 10) where a/d ratio is 0.7. The failure was characterised by crushing of concrete in the compression strut as evidence in the compressive damage (Fig. 10a). Although the initial diagonal crack along the compression struts continue to propagate as the loading steps increase (Fig. 10b), it was not deep enough to cause the collapse of the beams due to the presence of the web reinforcements. The rate of the propagation of the tensile crack also reduces with increasing quantity of web reinforcements. Evidence from the stress distribution in the reinforcements (Fig. 10c) buttressed the fact that the horizontal web reinforcement is more effective at low shear spans.

Compression strut failure could be attributed to the transverse compressive stress that exists between the loaded points and the support points [9], [28]. The transverse stress is more effective at low shear

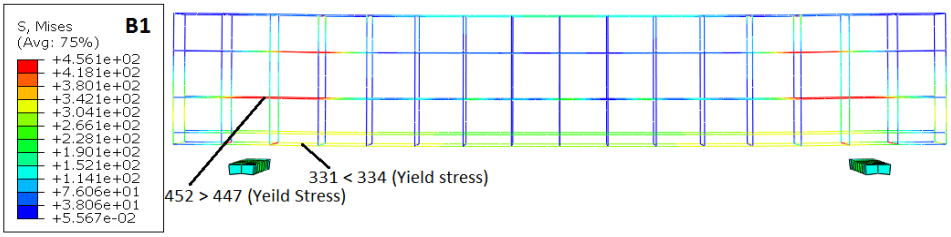
spans due to the steepness of the compression strut. Crushing of concrete occurs where the transverse compressive stress is higher than the concrete strength mostly at stress concentrations such as support and loaded points leading to abrupt termination of the analysis. Compression strut failure is mostly influenced by shear span to effective depth ratio and concrete compressive strength.



a. compressive damage in concrete



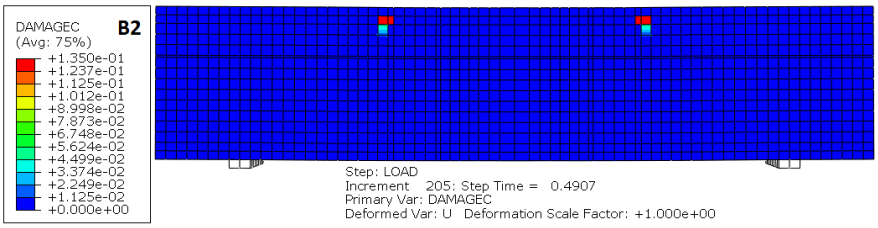
b. Tensile damage in concrete



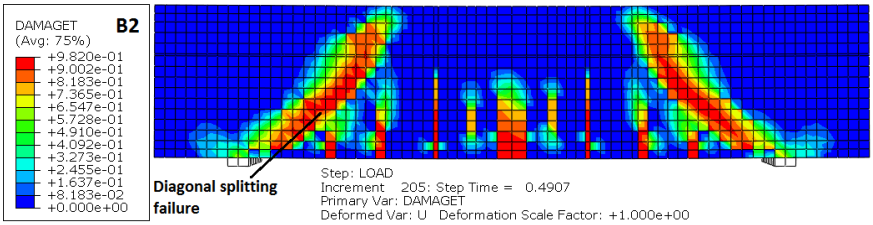
c. Stress distribution in reinforcement

Fig. 10: Shear Compression failure in specimen B1

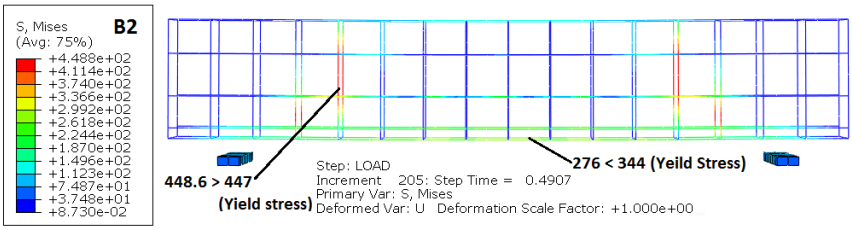
Diagonal Tension Failure. This is the most common mode of failure observed in the studied deep beam specimens. It occurred in ten (10) out of the eighteen (18) specimens tested. The failure mode was characterised by diagonal tensile damage along the compressive strut as well as yielding of web reinforcements crossing the struts. The failure is associated with the principal tensile stresses perpendicular to the compression struts. At initial loading steps, flexural cracks first appeared in the mid span region. The flexural cracks did not grow significantly as the analysis progresses since the tensile reinforcement is enough to allow development of full arch action mechanism. Further loadings increased the resultant principal stresses in the beams until the limiting tensile strength perpendicular to the compression strut is exceeded. Hence, the diagonal splitting failure occurred.



a. compressive damage in concrete



b. Tensile damage in concrete

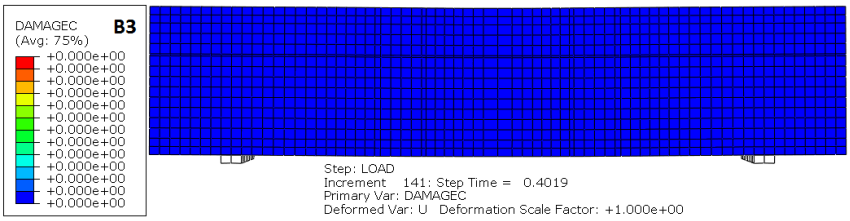


c. Stress distribution in reinforcement

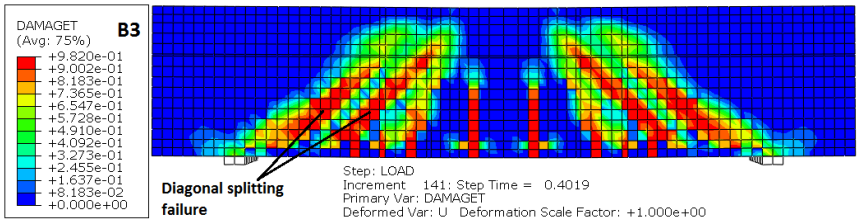
Fig. 11: Diagonal splitting failure in specimen B2

Some variables influence the occurrence of diagonal tension failure in deep beams. These include shear span - effective depth ratio, concrete strength, web reinforcement ratio and tensile reinforcement ratio. All the deep beams with a/d ratio of 1.4 failed in diagonal tension irrespective of the web reinforcement distribution and concrete strength. Typical diagonal splitting failure in specimens with a/d ratio of 1.4 is shown in Fig.s 11. The diagonal splitting is characterised by yielding of web reinforcements (Fig. 11c) and cracking of concrete along the compression struts (Fig. 11b). The final diagonal splitting is also accompanied with crushing of concrete in the nodal zones as seen in Fig. 11a. The amount of compressive damage at the nodal zones depends on the web reinforcement distributions. Similar failure modes have been observed in related studies [1], [28].

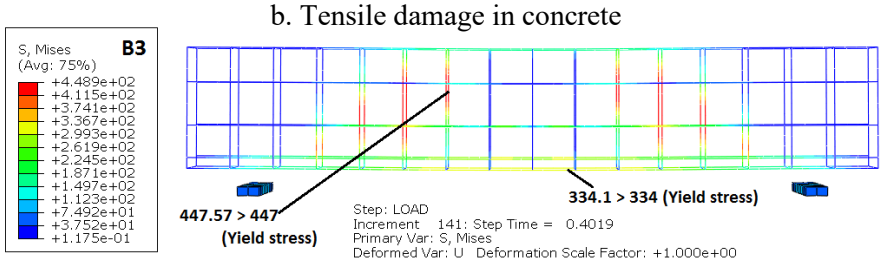
Where a/d ratio is at the specified limit of 2.0 for deep beams (ACI 318M, 2014), the failure mode of deep beam is somewhat between diagonal splitting and flexural shear failure depending on the web reinforcement ratio, tensile reinforcement ratio and concrete compressive strength. For high strength deep beams (specimens B3 and B6, Fig. 12) with low vertical web reinforcement ratio (R_v = 0.31%), the beam failed by diagonal splitting characterised by yielding of vertical web reinforcements and diagonal tensile cracking in concrete. The yielding of tensile reinforcement and crushing of concrete have not occurred (Fig. 12a and 12c). This is because the developed principal tensile stresses in the shear span is beyond the limits that could be resisted by the combined influence of web reinforcement and concrete tensile strength. Further strengthening of the beam in shear by increasing the web reinforcement ratio will alter the failure mode as noticed in specimens B9 and B12 (see next section) since the developed stress in the tensile reinforcements at failure is already close to the yield value.



a. compressive damage in concrete



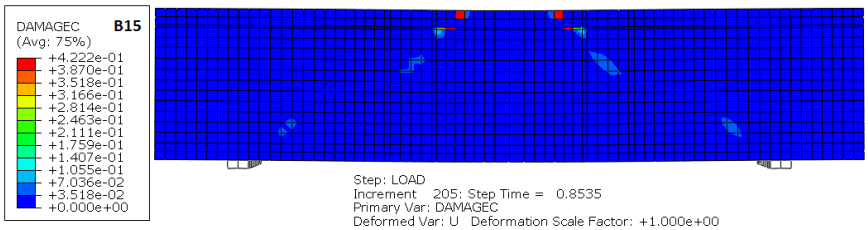
b. Tensile damage in concrete



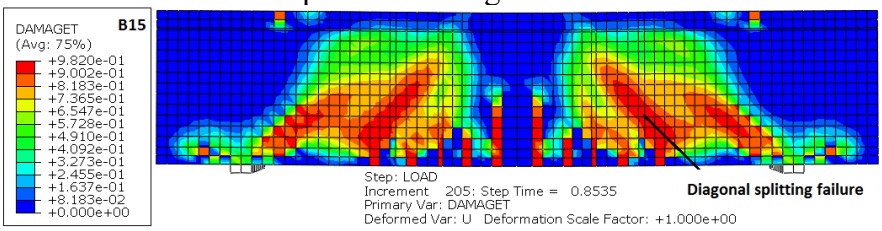
c. Stress distribution in reinforcement

Fig. 12: Diagonal splitting failure in specimen B3

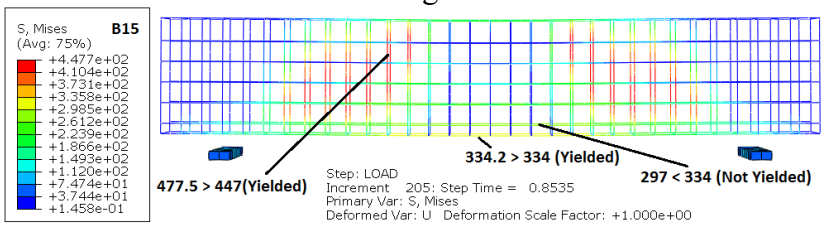
Unlike the high strength deep beams, analysis results of specimens B15 and B18 (Fig. 13) show that normal strength deep beams with a/d ratio of 2.0 failed in diagonal tension irrespective of web reinforcement distributions. This behaviour could be linked to the lower tensile strength in the normal strength beams since there is direct relationship between the compressive and tensile strength of concrete.



a. compressive damage in concrete



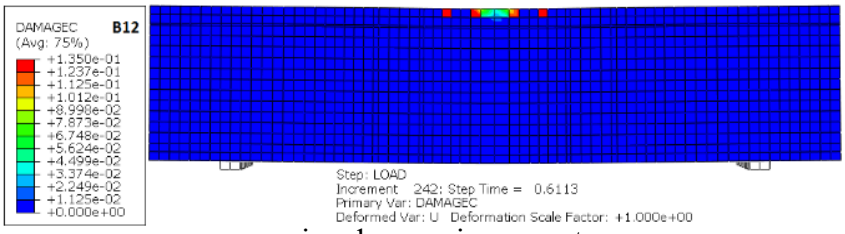
b. Tensile damage in concrete



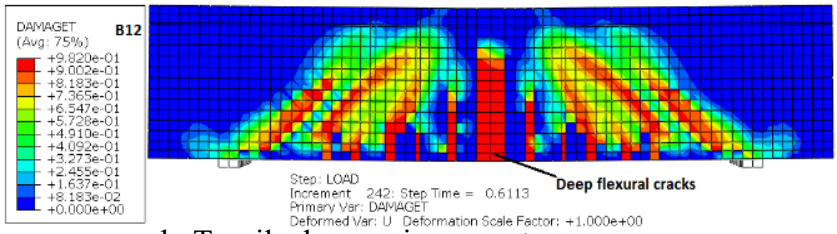
c. Stress distribution in reinforcement

Fig. 13: Diagonal splitting failure in specimen B15

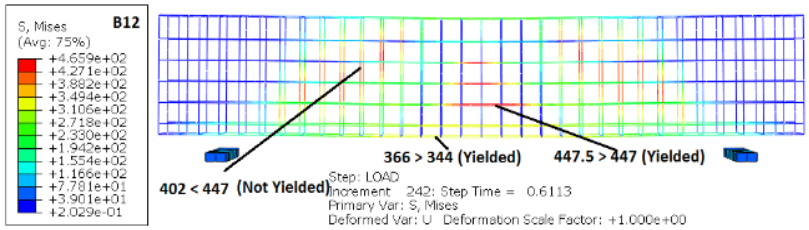
Flexural Shear Failure. This failure occurs when the flexural capacity is exceeded before the ultimate shear strength and flexural compression strength limits are reached as witnessed in specimens B9 and B12 (Fig. 14) where a/d ratio is 2.0 and Rv is substantially high (Rv = 0.63%). At initial loading stage, flexural cracks appeared close to the mid-span at the beams bottom. As the loading steps increase, more flexural cracks developed with accompanied diagonal tension cracks. However, the developed principal tensile stress in the shear span does not reach the limiting tensile strength due to the high Rv ratio in the beams. Final collapse occurred due to yielding of tensile reinforcement accompanied by excessive flexural cracks at the mid-span region (Fig.s 14b and 14c). Excess strain in the tensile reinforcement and the accompanied large deflection caused evolution of compressive damage in the compression zone as shown in Fig. 14a and yielding of web horizontal web reinforcement as seen in Fig. 14c. Hence, the failure of the compression zone and yielding of web reinforcement are post failure phenomenon.



a. compressive damage in concrete



b. Tensile damage in concrete



c. Stress distribution in reinforcement

Fig. 14: Flexural shear failure in specimen B12

Comparative Study

The result of the predicted shear strength of the eighteen deep beams for the five models considered in this study is presented in Table 7. As a means of preliminary inspection of the experimental data, a notched boxplot (Fig. 15) was obtained using the *ggplot2* library [31] of R software version 3.5.1 [27] to check for possible outliers and to visually compare the shear strength results from the five models, using Tukey's five number summaries [32], [33] including: minimum, lower-hinge, median, upper-hinge, maximum observation, respectively.

Table 7: Shear strengths of deep beams from FEM and STMs

Specimen	FEM (kN)	Strut and Tie Models (kN)			
		ACI 318M	EC 2	Arabzadeh	Al-Khafaji
B1	1524.0	621.0	412.0	723.0	677.0
B2	712.0	444.0	294.0	407.0	503.0
B3	630.0	332.0	220.0	236.0	425.0
B4	1417.0	621.0	412.0	723.0	851.0
B5	741.0	444.0	294.0	407.0	624.0
B6	665.0	332.0	220.0	236.0	501.0
B7	1315.0	621.0	412.0	723.0	730.0
B8	826.0	444.0	294.0	407.0	610.0
B9	689.0	332.0	220.0	236.0	577.0
B10	1289.0	621.0	412.0	723.0	905.0
B11	884.0	444.0	294.0	407.0	731.0
B12	715.0	332.0	220.0	234.0	653.0
B13	741.0	311.0	233.0	445.0	710.0
B14	625.0	222.0	167.0	250.0	626.0
B15	606.0	166.0	125.0	145.0	579.0
B16	832.0	311.0	233.0	445.0	657.0
B17	528.0	222.0	167.0	250.0	519.0
B18	497.0	166.0	125.0	145.0	428.0

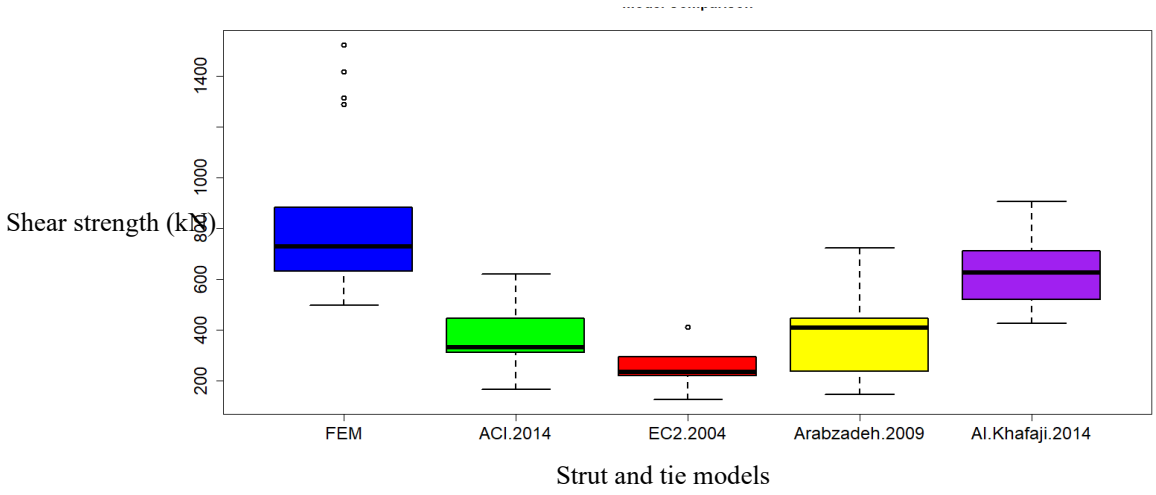


Fig. 15: Notched boxplots of shear strength of deep beams per model

The notch displays a confidence interval around the median which is normally based on the median +/- 1.58*IQR/sqrt(n) and are used to compare groups such that; if the notches of two boxes do not overlap, it is a strong evidence that the medians differ. The tick middle lines represent data median, the lower end of boxes denote data lower-hinge (lower quartile), the upper end is the upper-hinge (upper quartile), lower end of the vertical line through boxes denote minimum data value while the upper end of it denote maximum value, respectively.

It can be observed at a glance at the boxplots that FEM may achieve a significantly different shear strength prediction for deep beams than ACI 318M model, EC2 model and Arabzadeh's model, respectively, since FEM notch (box) is never intersecting with those of the three models. This may imply that median shear strength obtained by FEM is significantly different from those estimated by

the three strut and tie models while the latter models (FEM and Al-khafaji's model) achieved approximately the same median estimates for the sample deep beams. Although Al-khafaji strut and tie model's notch slightly overlaps with that of FEM, we cannot deterministically judge them to be the same until after a classical statistical test is conducted on the study data set.
Data evidences in Table 8 reject the null hypothesis of multivariate normality for the data, since test p-value 0.0075 is smaller than 5%. Therefore, a nonparametric equivalent of the one-way ANOVA called Kruskal-Wallis Rank Sum Test (K-WRST) according to [24] was adopted, using function *kruskal.test* in R software.

Table 8: Test of Multivariate Normality.

Test	H	p-value	MVN
Royston	10.07304	0.0075	NO

From the K-WRST results in Table 9, it is evident with 95% confidence that there is enough data evidence to reject H_0 of no statistically detectable difference among the median measurements of the shear strength of the deep beams by the methods. This inference is because the test p-value 9.354e-11 is smaller than the critical rejection region of 5%.

Table 9: Kruska-Wallis Rank Sum Test

Data	K-WRST Chis-squared	df	p-value
Shear strength of deep beams	52.807	4	9.354e-11

To determine, which particular models have significantly different median measurement of shear strength measurement, it is necessary to follow-up the K-WRST results with a post-hoc test, using the *pgirmess* library [34] of the R software at 95% significance level. In the post-hoc test, greater observed difference than critical difference indicates models involved have significantly different measurements.
Data evidences in Table 10 reveals that, with 95% confidence, FEM predicted shear strength of deep beams is significantly different form all strut and tie models except Al-Khafaji's model. This inference is further evident in that, Al-Khafaji's strut and tie model is also significantly different from the other three strut and tie models. The other three STMs (ACI 318M model, EC2 model and Arabzadeh's model) are obvious the same in terms of their efficiencies in determining shear strength of deep beams. All these inferences can be comprehended at a glance from Fig. 15.

Table 10: Post-hoc Test for Median of Shear Strength Measurement Difference

Pair of Models	Observed Difference	Critical Difference	Difference
FEM-ACI 318M, 2014	39.0556	24.4443	TRUE
FEM-EC2 (2004)	55.0556	24.4443	TRUE
FEM-Arabzadeh (2009)	37.5000	24.4443	TRUE
FEM-Al-Khafaji, 2014	11.4444	24.4443	FALSE
ACI 318M (2014)- EC2 (2004)	16.0000	24.4443	FALSE
ACI 318M (2014) –Arabzadeh (200)	1.5556	24.4443	FALSE
ACI 318M, 2014 –Al-Khafaji, 2014	27.6111	24.4443	TRUE
EC 2, 2004 - Arabzadeh, 2009	17.5556	24.4443	FALSE
EC 2, 2004- Al-Khafaji, 2014	43.6111	24.4443	TRUE
Arabzadeh, 2009 - Al-Khafaji, 2014	26.0556	24.4443	TRUE

Conclusions

From the results of numerical study conducted in this research, the followings are concluded:

(1) The diagonal cracking load generally decreased with increasing a/d ratio up to a/d limit of 1.5, for greater a/d ratio however, the trend depended on the web reinforcement distributions. Also, the ultimate strength and the load - deflection response of the beams generally reduced with increased a/d;

(2) The compressive strength of concrete (f_c) most significantly influenced the structural behaviour of the studied beams. The V_c and V_u increased by average of 42.00% and 30.40% respectively due to change in f_c from 26.05 N/mm^2 to 52.10 N/mm^2. The load-deflection responses were also higher in beams with greater f_c;

(3) The parametric effect of web reinforcements on V_u was strongly influenced by a/d ratio. It was found that increasing R_v and R_h ratio from 0.31% to 0.63% led to 13.00% and 4.80% reduction respectively in V_u for beams with a/d ratio of 0.7, while it led to average increment of 11.40% and 4.84% respectively for greater a/d ratio (a/d= 1.4 and 2.0). However, the influence of web reinforcements on V_c was erratic and minima. Also, change in R_h did not affect the load-deflection response of the beams while the slight improvement on the load deflection response due to change in R_v only occurred after the diagonal cracks have fully developed.

(4) It was also found that deep beams with a/d ratios of 0.7 and 1.4 failed in shear compression and diagonal tension respectively regardless of web reinforcement distributions and concrete compressive strength, while the failure modes varied somewhat between diagonal splitting and flexural shear failure depending on the web reinforcement ratio, tensile reinforcement ratio and concrete compressive strength for beams with a/d ratio of 2.0.

(5) Apart from Strut and Tie Model proposed by Al-Khafaji et al. [1], all the considered Strut and Tie Models under-predicted the ultimate load of RSCC deep beams.

Acknowledgements

This study was funded by the Federal Government of Nigeria through the TETFUND Institution-Based Research (IBR) allocation. The authors wish to express their deep appreciation for the support.

References

[1] J. Al-Khafaji, I. Al-Shaarbaf, and W. H. Sultan, "Shear Behavior of Self Compacting Concrete Deep Beams," *Journal of Engineering and Development*, vol. 18, no. 2, pp. 36–58, 2014.

[2] ACI 318M, *Building Code Requirements for Structural Concrete (ACI 318M-14) and Commentary (ACI 318RM-14)*. Farmington Hills, MI: American Concrete Institute, 2014.

[3] Eurocode 2, "Design of concrete structures - Part 1-1: General rules and rules for buildings." European Committee for Standardization, United Kingdom, 2004.

[4] G. Russo, R. Venir, and M. Pauletta, "Reinforced Concrete Deep Beams-Shear Strength Model and Design Formula," *ACI Structural Journal*, vol. 102, no. 3, pp. 429–437, 2005.

[5] J. Al-Khafaji, I. Al-Shaarbaf, and W. H. Sultan, "Shear Behavior of Fibrous Self Compacting Concrete Deep Beams," *Journal of Engineering and Development*, vol. 18, no. 16, pp. 36–58, 2014.

[6] L. T. Yaw, J. B. Osei, and M. Adom-Asamoah, "On The Non-Linear Finite Element Modelling of Self-Compacting Concrete Beams," *Journal of Structural and Transportation Studies*, vol. 2, no. 2, pp. 1–18, 2017.

[7] M. M. S. Anjitha and K. R. Kumar, "Analytical Studies on Hybrid Self Compacting Concrete Deep Beam Using Fem Software," *International Journal of Innovative Research in Science, Engineering and Technology*, vol. 4, no. 5, pp. 71–77, 2015.

[8] Q. Q. Liang, B. Uy, and G. P. Steven, "Performance-Based Optimization for Strut-Tie Modelling of Structural Concrete," *Journal of Structural Engineering*, vol. 128, no. 6, pp. 815–823, 2002.

[9] A. R. Mohamed, M. S. Shoukry, and J. M. Saeed, "Prediction of the behavior of reinforced concrete deep beams with web openings using the finite element method," *Alexandria Engineering Journal*, vol. 53, no. 2, pp. 329–339, 2014.

[10] A. Arabzadeh, A. R. Rahaie, and R. Aghayari, "A Simple Strut-and-Tie Model for Prediction of Ultimate Shear Strength of RC Deep Beams," *International Journal of Civil Engineering*, vol. 7, no. 3, pp. 141–153, 2009.

[11] Y. W. Choi, H. K. Lee, S. B. Chu, S. H. Cheong, and W. Y. Jung, "Shear Behavior and Performance of Deep Beams Made with Self-Compacting Concrete," *International Journal of Concrete Structures and Materials*, vol. 6, no. 2, pp. 65–78, 2012.

[12] Dassault Systèmes, *Abaqus 6.12 Analysis User 's Manual, Volume III: Materials*. Province: Dassault Systèmes Simulia Corp., Providence, 2012.

[13] Y. Sümer and M. Aktaş, "Defining parameters for concrete damage plasticity model," vol. 1, no. 3, pp. 149–155, 2015.

[14] A. Demir, H. Ozturk, and G. Dok, "3D Numerical Modeling of RC Deep Beam Behavior by Nonlinear Finite Element Analysis," *Disaster Science and Engineering*, vol. 2, no. 1, pp. 13–18, 2016.

[15] J. Lubliner, J. Oliver, S. Oller, and E. Oñate, "A Plastic-Damage Model for Concrete," *International Journal of Solids and Structures*, vol. 25, pp. 299–329, 1989.

[16] J. Lee and G. L. Fenves, "Plastic-Damage Model for Cyclic Loading of Concrete Structures," *Journal of Engineering Mechanics*, vol. 124, no. 8, pp. 892–900, 1998.

[17] M. A. Akinpelu and A. A. Adedeji, "Structural Response of Reinforced Self - Compacting Concrete Deep Beam using Finite Element Method," *Journal of Soft Computing in Civil Engineering*, vol. 2, no. 1, pp. 33–58, 2018.

[18] S. Michał and W. Andrzej, "Calibration of the CDP model parameters in Abaqus," in *The 2015 World congress on Advances in Structural Engineering and Mechanics (ASEM15)*, 2015.

[19] T. Jankowiak and T. Odygowski, "Identification of Parameters of Concrete," *Foundation of Civil and Environmental Engineering*, no. 6, pp. 53–69, 2005.

[20] A. S. Genikomsou and M. A. Polak, "Damaged plasticity modelling of concrete in finite element analysis of reinforced concrete slabs," in *9th International Conference on Fracture Mechanics of Concrete and Concrete Structures*, 2016.

[21] B. . Welch, "On the comparison of several mean values: an alternative approach," *Biometrika*, vol. 38, pp. 330–336, 1951.

[22] J. P. Royston, "An Extension of Shapiro and Wilks W Test for Normality to Large Samples," *Applied Statistics*, vol. 31, no. 2, pp. 115–124, 1982.

[23] S. Korkmaz, D. Goksuluk, and G. Zararsiz, "MVN: An R Package for Assessing Multivariate Normality," *The R Journal*, vol. 6, no. 2, pp. 151–162, 2014.

[24] M. Hollander and D. A. Wolfe, *Nonparametric Statistical Methods*. New York: John Wiley & Sons, 1973.

[25] R. G. Miller, *Simultaneous Statistical Inference*, 2nd Editio. Verlag, New York: Springer, 1981.

[26] B. S. Yande, *Practical data analysis for designed experiments*. New York: CRC Press, 1997.

[27] R Core Team, "R: A language and environment for statistical computing," 2018. [Online]. Available: https://www.r-project.org/.

[28] F. K. Kong, *Reinforced Concrete Deep Beams*. New York: Taylor & Francis Books, Inc., 2002.

[29] M. Mohammadhassani, Z. M. Jumaat, A. Ashour, and M. Jameel, "Failure modes and serviceability of high strength self compacting concrete deep beams," *Engineering Failure Analysis*, vol. 18, pp. 2272–2281, 2011.

[30] M. Mohammadhassani, M. Z. Jumaat, M. Jameel, H. Badiee, and A. M. S. Arumugam, "Ductility and performance assessment of high strength self compacting concrete (HSSCC) deep beams : An experimental investigation," *Nuclear Engineering and Design*, vol. 250, no. 2, pp. 116–124, 2012.

[31] H. Wickham, *ggplot2: Elegant Graphics for Data Analysis*. New York: Springer-Verlag, 2016.

[32] J. W. Tukey, "Exploratory Data Analysis," in *Section C*, 1977.

[33] R. McGill, J. W. Tukey, and W. A. Larsen, "Variations of box plots," *The American Statistician*, vol. 32, pp. 12–16, 1978.

[34] P. Giraudoux, "pgirmess: Spatial Analysis and Data Mining for Field Ecologists. R package version 1.6.9.," 2018. [Online]. Available: https://cran.r-project.org/package=pgirmess.